Ocean Engineering 195 (2020) 106657

Contents lists available at ScienceDirect

Ocean Engineering

journal homepage: www.elsevier.com/locate/oceaneng

The prediction of ship added resistance at the preliminary design stage by the use of an artificial neural network

Tomasz Cepowski

Faculty of Navigation, Maritime University of Szczecin, Szczecin, Poland

ARTICLE INFO

Keywords:
Ship design
Added resistance
Artificial neural network
Preliminary design
Approximation
Model tests
Head waves

ABSTRACT

This article focuses on the use of an artificial neural network to estimate added resistance in regular head waves while using ship design parameters, such as length, breadth, draught or Froude number. In order to create a reliable model, only experimental data determined through model test measurements was used to train the neural network. This study showed that added wave resistance values predicted by the neural network soundly correlated with measured data and had good generalization ability. The developed neural network was presented in the form of mathematical function. This article presents examples of the use of this function to calculate added wave resistance. Functions presented here could have practical application in ship resistance analysis at the preliminary design stage.

1. Introduction

A ship is designed in many stages, such as concept design, preliminary design, contract design and detailed design. The hull line plan, ship general arrangement and propulsion system are conceptualised at the preliminary design stage (Chądzyński, 2001), with this design stage consisting of parametric and geometric design phases. Watson (1998), Rawson and Tupper (2001), Papanikolaou (2014) argue that the purpose of the parametric design is, among others to estimate main propulsion and powering parameters. In order to accurately estimate these parameters, expert knowledge relating to total hull resistance is required. It was also noted (Arribas and Pérez, 2007, Papanikolaou, 2014) that total hull resistance includes added wave resistance, which:

- is connected with ship seaway in storm waves,
- can contribute to around 30–50% of total ship resistance,
- can lead to a remarkable drop in operating speed,
- depends on, among other factors, hull dimension and shape.

Added wave resistance can be determined through model test measurements or far- or near-field numerical methods. Far-field methods are most often based on momentum conservation theory (Maruo, 1960; Joosen, 1966 and Newman 1967) and the radiated energy approach (GERRITSMA and BEUKELMAN, 1972). Near-field numerical methods are based on pressure integration over a wetted hull surface and include approaches developed by Fujii and Takahashi (1975), SALVESEN (1978), FALTINSEN et al. (1980), Joncquez et al. (2008), Kuroda et al. (2008) and Kim and Kim (2011). Kashiwagi (2009) found satisfactory results using an enhanced unified theory using a modified approach by Maruo.

Approximation methods based on semi empirical formulas were also used to estimate additional resistance. The common methods are STAWAVE-1 I STAWAVE-2 that have been developed by the Sea Trial Analysis-Joint Industry Project (Boom et al., 2013) and implemented by The International Towing Tank Conference in (ITTC, 2017). The STAWAVE-1 method estimates the added resistance of irregular waves caused by short head wave reflection, which depends on the waterline shape in the bow region. This method was developed for large ships with a high forward speed within trial conditions in mild waves. The STAWAVE-2 method was developed to approximate the transfer function of the added resistance in heading regular waves by using main ship characteristics. The sea keeping model test results from 200 ships were utilised to develop this method. The transfer function calculated by the use of STAWAVE-2 takes the mean resistance increase due to wave reflection and the motion induced resistance (ITTC, 2017) into account. Due to simple mathematical form and high accuracy, both STAWAVE methods are commonly used to estimate the added resistance and accuracy compare other methods.

Liu and Papanikolaou (2016a, 2016b), developed various simple semi-empirical formulations for the rapid estimation of ship added resistance in head waves. They considered the effect of ship hull form characteristics, with best fitting from available experimental data for

E-mail address: t.cepowski@am.szczecin.pl.

https://doi.org/10.1016/j.oceaneng.2019.106657
Received 8 May 2019; Received in revised form 22 October 2019; Accepted 27 October 2019
Available online 13 November 2019

various types of hull forms. Liu et al. (2016) further refined this research for simple use in engineering applications. Liu and Papanikolaou (2019) extended their previously developed formulas for the approximation of added resistance at wider speed ranges, and introduced a new parameter based on B/T and investigated trim effect after conducting an extensive parametric study to capture the influence of draft on added resistance.

The author of this paper (Cepowski, 2008) developed an approximation function for the estimation of an added wave resistance coefficient on the basis of containership design parameters. The length between perpendiculars/breadth ratio, breadth/draught ratio and block and waterline coefficient were taken into account as hull design parameters in this study. Recently, the author (Cepowski, 2016) applied an artificial neural network to predict added wave resistance transfer function for bulk carriers thought the use of waterplane area and coefficient, as well as ship speed and regular wave frequency.

Considering all of the above methods, model tests were found to be the most reliable and accurate. Though model tests are both expensive and time-consuming, and also require a hull form. Computational fluid dynamics (CFD) methods are considered to be the most accurate calculation methods, though these methods are also time-consuming and require detailed hull form data.

Alternatively, approximation methods were found to be the least accurate, but can be applied at the conceptual design stage, where a detailed hull form is not available. These methods can be also applied to multi-criteria design parameter optimization using genetic algorithms, due to their simple mathematical form. The main disadvantages of approximation methods are that they are only applicable for conventional ships that have been tested and examined. These methods cannot be applied in the case of innovative modern ship design.

The majority of the above methods are limited to resistance calculations for a head wave. Usually, the mean added wave resistance is calculated by the use of a wave system according to the superposition principle. Then, applying this principle, an increase in the statistical mean resistance R_{AW} in irregular wave is calculated as:

$$\boldsymbol{R_{AW}} = 2\int_0^\infty \boldsymbol{R(\omega)S_{\zeta\zeta}(\omega)d\omega} \tag{1}$$

where:

R_{AW} – statistical mean wave resistance increase
R – added resistance from the regular wave,
ω –frequency,
$S_{\zeta\zeta}$ - wave energy spectrum density function.

Full scale added resistance due to waves R may be reduced to the non-dimensional coefficient (ρ_{AW}) by the following equation:

$$\boldsymbol{C_{AW}} = \frac{R}{\boldsymbol{\zeta_a^2 \rho g \frac{B^2}{L}}} \tag{2}$$

where:

C_{AW} – non-dimensional added wave resistance coefficient,
ζ_a – amplitude of a regular wave,
B – ship breadth,
L – ship length,
ρ – seawater density,
g – acceleration due to gravity.

A selection of main dimensions in the case of additional wave resistance is the most effective method in parametric design. A body line plan is required to estimate the non-dimensional added wave resistance coefficient through the use of model tests or numerical methods. Though, an accurate estimate of the additional resistance of a ship at the parametric design can be problematic because the hull line plan is not developed at this stage.

Therefore, the aim of this research was to develop a simple, accurate function to estimate the non-dimensional added wave resistance coefficient by the use of the ship design parameters such as length, breadth, draught or Froude number. In order to discover a reliable model, only measurement results through the use of model tests were used in this research. In this study, the estimation of added wave resistance was only limited to head waves.

2. Research method

A key element of this research was to determine the function which would estimate the non-dimensional added wave resistance coefficient based on design parameters and wave frequency equivalent:

$$\boldsymbol{C_{AW}} = \boldsymbol{f(LBP, B, d, CB, Fn, \lambda / LBP)} \tag{3}$$

where:

LBP – length between perpendiculars,
B – breadth,
d – draught,
CB – block coefficient,
Fn – Froude number,
λ/LBP –the wavelength/ship length ratio,
f - function for estimating the added ship resistance coefficient.

To determine f function, measured added wave resistance values were approximated by the use of artificial neural networks. In recent years, artificial neural networks (ANN) have been used in a number of scientific ship design theory publications. Abramowski (2013) applied artificial neural networks for the optimization of design parameters in cargo ships. A mathematical model to determine the effective power of a ship was developed by the use of neural networks in this publication. Gurgen et al. (2018) applied an artificial neural network to predict the main dimensions of chemical tankers. Main ship parameters, such as, overall length, length between perpendiculars, breadth, draught and freeboard were etimated on the basis of deadweight and vessel speed in this paper. Gurgen et al. (2018) argued that the initial main particulars of chemical tankers could be determined through the use of ANN, offering levels which were much more accurate than compared to sample ship data. Ekinci et al. (2011) used 18 computational intelligence methods (including neural network methods) to estimate the main design parameters of oil/chemical tankers. In many scientific studies, the use of artificial neural networks offers excellent results.

3. Artificial neural networks

Artificial neural network theory is based on the analysis of a biological nervous system. A biological nervous structure consists of neurons and their connections. A mathematical model of a neural network is created, based on this structure and signal transmission. This model was built from an input, output and one or more hidden layers that consist of neurons (Haykin, 1994). Values from previous layers are passed through neurons ($x_1, x_2, \ldots, x_n$) in an artificial neuron which were connected with weights ($w_1, w_2, \ldots, w_n$) as followed (and shown in Fig. 1):

$$y = \varphi\left(\sum_{i=0}^{n} w_i \cdot x_i\right) \tag{4}$$

where:

x_i – input signal,
y – neuron output signal,
w_i – weights, w_0 – bias,
φ – activation function.

The sum result value was transmitted to the node output value by the

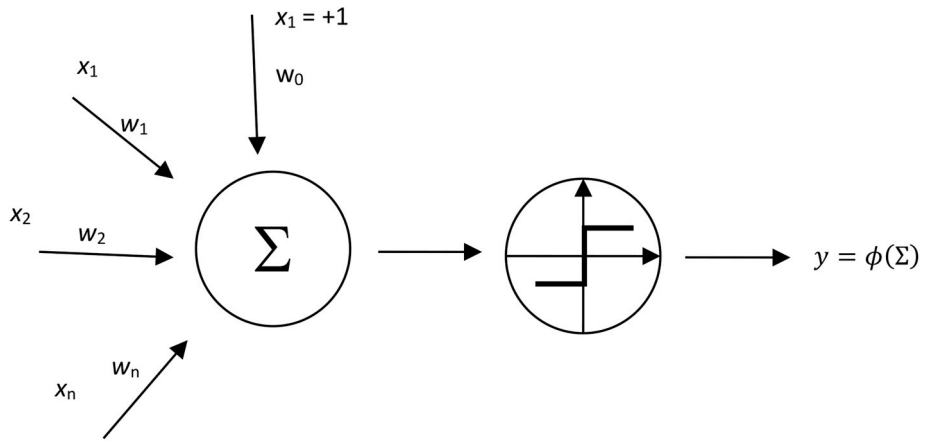

Fig. 1. Signal processing in an artificial neuron, where:
x_i – input signal, y – neuron output signal, w_i – weights, w_0 – bias, ϕ – activation function.

use of an activation function. A number of functions are often used as activation functions in the hidden layer and the output layer. In this study, the following activation function were used:

- purelin (where the neuron activation is passed on directly as the output):

$$y = x \tag{5}$$

- standard logistic function:

$$y = \frac{1}{1 + \exp(-x)} \tag{6}$$

- hyperbolic tangent:

$$y = \frac{\exp(a) - \exp(-a)}{\exp(a) + \exp(-a)} \tag{7}$$

After the learning process, an artificial neural network maps the input vector X to resulting vector Y:

$$f : X \rightarrow Y \tag{8}$$

The aim of the learning process is to calculate the weight value *wi*, where the network response is consistent with the results. Weight w_i are calculated on the basis of input and output data.

The main problems in developing and training an artificial network are selecting the optimal network structure and calculating neuron weight values. Therefore, different types of neural network structure and learning methods can be used.

A multilayer perceptron (MLP), consisting of an input, hidden and output layer, as well as utilising a backpropagation learning algorithm is often applied in regression problems.

Overfitting phenomenon is the main problem in neural networks learning. This phenomenon occurs when a model has too many variables in relation to the data sample size. A test set method is usually used to detect and avoid this phenomenon. Unfortunately, about 30–50 percent of randomly selected data is wasted throughout the neural network development process to test and validate the model in this method.

In this study, the search process for the best neural network went through the following steps:

- creating a neural network topology,
- training and testing the network,
- an accuracy assessment through the use of test results.

The following standardized parameters were used for accuracy assessment:

- Pearson correlation coefficient (PCC):

$$\mathbf{PCC} = \frac{\sum(\rho - \overline{\rho})(\rho_e - \overline{\rho_e})}{\sqrt{\sum(\rho - \overline{\rho})^2(\rho_e - \overline{\rho_e})^2}} \tag{9}$$

- Mean squared error (MSE):

$$\mathrm{MSE} = \frac{\sum(\rho - \rho_e)^2}{2n} \tag{10}$$

where:

ρ –added ship resistance coefficient from the data set,
ρ_e – estimated added ship resistance coefficient through the use of a neural network,
n – number of records in the data set.

To develop a neural network the following assumptions were made:

- sum of square error function (SOS) as an error function,
- Backpropagation (Fausett, 1994; Haykin, 1994; Patterson, 1996), Conjugate Gradient Descent (Bishop, 1995), Levenberga-Marquardt (Bishop, 1995; Shepherd, 1997), Broyden-Fletcher-Goldfarb -Shanno (Broyden, 1970; Fletcher, 1970; Shanno, 1970; Goldfarb, 1970; Bishop, 1995; Shepherd, 1997) algorithms as a training method,
- linear, logistic or hyperbolic tangent function as activation,
- the training, validation and test sets include 227, 113 and 114 cases, respectively.

Ship models of wide design characteristic ranges available in literature were used in this study to:

- obtain the most universal predictive model,
- check whether neural networks would provide accurate solutions in this case.

The measurement data of the added ship resistance coefficient on regular wave of 14 model ships was used. The data source was experimental research carried out by GERRITSMA and BEUKELMAN (1972), Strøm-Tejsen (1973), Journee (1976), Nakamura (1976), Kadomatsu (1988), Guo and Steen (2010), Sadat-Hosseini et al. (2013), Ley et al. (2014), Simonsen et al., 2014, Söding et al. (2014) and Sprenger et al.

(2015). The design characteristics of ship models are presented in Table 1. This table shows that length between perpendiculars, breadth, draught, block coefficient and Froude number values are of relatively wide ranges. However:

- the upper and lower boundaries of the LBP/B ratio (equals from 5.05 to 7.5) are rather too narrow - according to ship design theory (Papanikolaou, 2014) the LBP/B ratio range for merchant ships is 4.5–8.5.
- the lower boundary of the B/d ratio which equals 2.49 is rather to high - according to ship design theory (Papanikolaou, 2014) the range for merchant ships of the B/d ratio starts from 2.1 to 4.

These boundaries limit the method application, because a neural network usually has poor ability to extrapolate for input values outside the training ranges.

4. Results and discussion

In this study, artificial neural networks were trained and tested by the use of Statistica software (TIBCO, 2017). The following neural network types were tested for the prediction of an added wave resistance coefficient:

- generalized regression neural network (GRNN),
- multilayer perceptron (MLP),
- Radial basis function network (RBF),
- Linear network.

Length between perpendiculars, breadth, draught, block coefficient, Froude number Fn and non-dimensional wave frequency equivalent were used as the input layer and a measured non-dimensional added wave resistance coefficient was used as the output layer in the neural networks.

In order to acquire the closest output values to the measured data, various numbers of neurons in the hidden layer and training methods were tested. For the GRNN neural network, the number of neurons in the first hidden layer was equal to the number of training cases, i.e. 227.

Table 2 shows MSE error values for different hidden neurons and teaching algorithms of the developed neural networks with respect to experimental data, and were broken down into:

- data used for network training – the training set,
- data used for network validating during training – the validation set,
- data used only for network testing – the test set.

Table 2
Overview of the different neural network types, where: BP - Error back propagation algorithm, CG - Conjugate gradient algorithm, BFGS – Broyden-Fletcher-Goldfarb-Shanno algorithm, KM - K-Means algorithm, KN – K-Nearest Neighbour algorithm, PI Pseudo-Inverse algorithm and SS - sub-Sample algorithm.

Network type	Number of hidden neurons	Training method/ number of training epochs	MSE Error [-]		
			Training set (227 cases)	Validation set (113 cases)	Test set (114 cases)
MLP[a]	6	BP/50,CG/ 631	1.02	0.98	1.10
MLP	4	BP/50,CG/ 618	1.08	0.99	1.11
MLP	9	BP/50,CG/ 718	0.97	0.97	1.11
MLP	10	BFGS/209	0.61	1.09	1.12
MLP	7	BFGS/141	0.66	1.01	1.17
MLP	3	BP/50,CG/ 871	1.12	1.02	1.17
MLP	2	BP/50,CG/ 630	1.22	1.13	1.21
MLP	7	BFGS/124	0.71	1.09	1.30
MLP	11	BFGS/169	0.70	1.04	1.36
MLP	5	BFGS/158	0.80	1.10	1.37
GRNN	227x2	SS	0.95	1.64	1.61
GRNN	227x2	SS	0.95	1.64	1.61
RBF	51	KM,KN,PI	1.43	1.63	1.77
RBF	45	KM,KN,PI	1.50	1.73	1.80
RBF	65	KM,KN,PI	1.48	1.77	1.84
RBF	50	KM,KN,PI	1.49	1.66	1.87

[a] found to be the best neural network for research.

The network which offers the smallest testing error is usually referred to as the best neural network. It can be observed from Table 2 that the minimum errors were found in the test set when 6 hidden nodes were chosen and Back propagation and Conjugate gradient algorithms were used. This table also shows that the BFGS algorithm enabled the network to be quickly trained, even with the use of only 124 training epochs. But this training method leads to large differences in error values in training and test sets. For example, MSE error values of best neural network training together with the use a BFGS algorithm were calculated as 0.61, 1.09 and 1.12 for training, validation and test sets. This can result in the phenomenon of overfitting and an inability to generalize data.

From among all the network types, the best solution was obtained when using the MLP neural network, with the following structure: 6 neurons in the input layer, 6 neurons in the hidden layer, and 1 neuron in the output layer. The structure of this neural network is graphically

Table 1
The design characteristics of ship models used in the research, where: LBP – length between perpendiculars, B – breadth, d – draught, CB – block coefficient and Fn – Froude number.

Model	LBP [m]	B [m]	d [m]	CB [-]	Fn [-]	LBP/B	B/d	Data source
Van der stel	152.5	22.8	9.14	0.563	0.15 0.2 0.25 0.3	6.69	2.49	GERRITSMA and BEUKELMAN (1972)
			5.2	0.503	0.15 0.2 0.25 0.3	6.69	4.38	Journee (1976)
S175 containership	175	25.4	8.5	0.559	0.15 0.2 0.25 0.3	6.89	2.99	Nakamura (1976)
Series 60 CB = 0.6	121.96	16.254	6.492	0.6	0.266 0.283	7.50	2.50	Strøm-Tejsen (1973)
Series 60 CB = 0.65	121.96	16.816	6.73	0.65	0.237 0.254	7.25	2.50	
Series 60 CB = 0.7	121.96	17.42	6.97	0.7	0.207 0.222	7.00	2.50	
Series 60 CB = 0.75	121.96	18.062	7.22	0.75	0.177 0.195	6.75	2.50	
Series 60 CB = 0.8	121.96	16.254	6.492	0.8	0.147 0.165	7.50	2.50	
WILS II containership	324	48.4	15	0.602	0.183	6.69	3.23	Söding et al. (2014)
DTC containership	355	51	14.5	0.661	0.139	6.96	3.52	Sprenger et al. (2015)
Cruise ship	220.32	32.04	7.2	0.654	0.223	6.88	4.45	Ley et al., (2014),
Bulk carrier	285	50	18.5	0.829	0.1 0.15	5.70	2.70	Kadomatsu (1988)
RoPax	90	17.82	4.2	0.549	0.087	5.05	4.24	Sprenger et al. (2015)
KVLCC2 tanker	320	58	20.8	0.808	0.142	5.52	2.79	Guo and Steen (2010); Sadat-Hosseini et al. (2013)
KRISO containership	230	32.2	10.8	0.651	0.26	7.14	2.98	Simonsen et al. (2014)
Min	90	16.254	4.2	0.503	0.087	5.05	2.49	–
Max	355	58	20.8	0.829	0.3	7.5	4.45	–

shown in Fig. 2.

The mathematical form of the neural network developed is given in the following relations:

$$C_{AW} = \frac{c + 0.01087}{0.08361} \tag{11}$$

where.

C_{AW} - the approximate non-dimensional added wave resistance coefficient [-],

c – variable calculated from the relation:

$$c = [3.2352 - 1.5865 - 3.5529 - 0.8379 - 0.8081 \;\; 0.8799] \times A + 1.23 \tag{12}$$

where:

A – column matrix:

$$A = \begin{bmatrix} \frac{1}{1+e^{-a_1}} \\ \frac{1}{1+e^{-a_2}} \\ \frac{1}{1+e^{-a_3}} \\ \frac{1}{1+e^{-a_4}} \\ \frac{1}{1+e^{-a_5}} \\ \frac{1}{1+e^{-a_6}} \end{bmatrix} \tag{13}$$

where:

$$\begin{bmatrix} a_1 \\ a_2 \\ a_3 \\ a_4 \\ a_5 \\ a_6 \end{bmatrix} = \begin{bmatrix} 3.966 & -2.399 & 3.903 & -0.313 & 1.244 & 1.314 \\ -0.771 & 1.832 & -1.256 & -0.085 & 1.242 & 0.983 \\ -2.361 & 2.803 & -1.692 & 1.452 & 0.706 & 3.916 \\ -0.784 & -3.674 & -0.801 & 4.763 & -0.922 & 0.146 \\ -2.206 & 0.078 & -2.305 & -3.661 & -1.082 & -4.008 \\ 16.057 & -1.270 & 12.316 & 3.231 & 3.893 & 3.88 \end{bmatrix} \times \begin{bmatrix} b_1 \\ b_2 \\ b_3 \\ b_4 \\ b_5 \\ b_6 \end{bmatrix} - \begin{bmatrix} 4.608 \\ 0.783 \\ 3.792 \\ -0.399 \\ -1.865 \\ -0.395 \end{bmatrix} \tag{14}$$

where:

$$b_1 = LBP \cdot 0.0038 - 0.3396 \tag{15}$$

$$b_2 = B \cdot 0.0240 - 0.3894 \tag{16}$$

$$b_3 = d \cdot 0.0602 - 0.2530 \tag{17}$$

$$b_4 = CB \cdot 3.0675 - 1.5429 \tag{18}$$

$$b_5 = Fn \cdot 4.6948 - 0.4085 \tag{19}$$

$$b_6 = \lambda/LBP \cdot 0.4425 - 0.0708 \tag{20}$$

where LBP is the length between perpendiculars (m), B is the breadth (m), d is the draught (m), CB is the block coefficient (−), Fn is the Froude number (−), λ/LBP is the wavelength/ship length ratio) (−).

The author developed a computer program called AddedResistance (Cepowski, 2019) for the calculation of added resistance utilising this algorithm. Fig. 3 shows the main form of this software. Lazarus IDE software (Lazarus, 2019) with a Free Pascal compiler was used to develop the AddedResistnace program.

MSE error values of the most effective neural network developed are presented in Table 2 and were calculated as 1.02, 0.98 and 1.1 for training, validation and test sets. These values are relatively low. Statistics for the test set are particularly important, as the data in this set was not used to develop the network, only test it. The test set statistic values testify to the ability of this network to generalize new cases. The MSE error values for test data vary slightly from training and validation set statistics. Regression between the estimated and measured values through the use of ANN is shown in Fig. 4. Pearson correlation coefficient values were calculated as 0.93, 0.93, 0.92 and 0.93 for training, validation, test and all data-sets, respectively. These results indicate that the measures and estimated values are all consistent. As a result, the developed neural network is probably not overfitted and could have good generalization ability.

Fig. 5 shows an error histogram for the training, validation, test and all sets, respectively. The error value indicates the difference between the measured and estimated value. This figure indicates that the largest portion of data coincided with a zero error line in the error range from −1.2 to 1.2 for all sets.

Figs. 6–10 compare added resistance data measured by model tests with values calculated using formula (11) and the STAWAVE-2 method (ITTC, 2017), as a function of wavelength/ship length ratio. These figures show that the neural network predicted relatively accurate results with the measured data. The transfer functions estimated by using the neural network have similar trends as did the functions estimated by using STAWAVE-2 method. Figs. 6 and 8 show that the neural network generates good approximation, even when a measured data set has a large dispersion.

A major drawback of neural networks is a poor ability to extrapolate. This means that testing and validation of neural network is more important and demanding than for a physics-based method. Fig. 11 shows a comparison of the values estimated by using a neural network with experimental data for test cases that were not at all used in the training of the neural network. This method, known as a “test set method”, is commonly used to assess the accuracy of a neural network in the process of its development.

In addition, the neural network was tested for ships that were not used at all in the development of the neural network. The design characteristics of these ship models are presented in Table 3. Fig. 12 shows a comparison of the values estimated by using the neural network and the STAWAVE-2 method with experiments for these ships.

These graphs indicate that the neural network effectively predicted data that was not used in the learning of the network. This confirms the

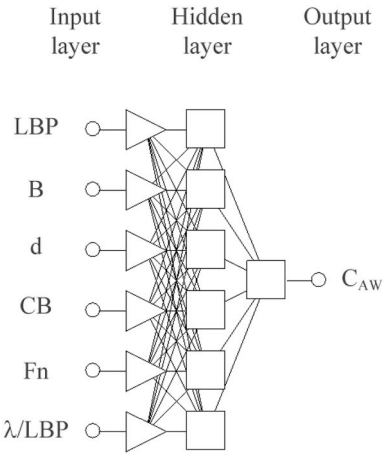

Fig. 2. Structure of the artificial neural network, where: LBP – length between perpendiculars, B – breadth, d – draught, Fn – Froude number, λ/LBP – the wavelength/ship length ratio, C_{AW} - non-dimensional added wave resistance coefficient.

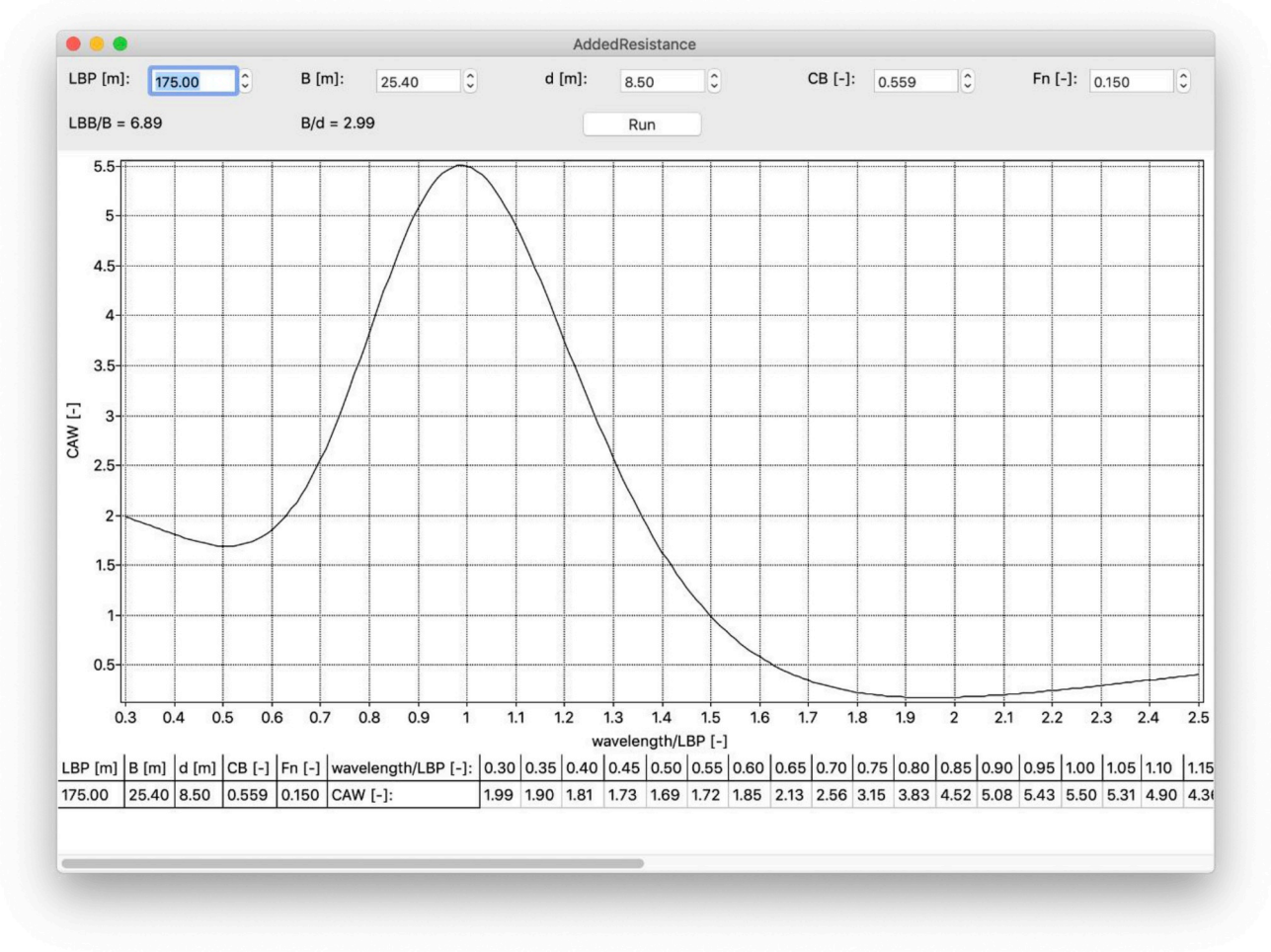

Fig. 3. The main form of "AddedResistance" software (Cepowski, 2019).

generalization capability of the developed neural network.

5. Example calculation

This section of the article presents an example of the practical use of the developed neural network for calculating the added wave resistance coefficient C_{AW}. The calculations were performed under the following assumptions:

- ship length between perpendiculars LBP = 152.5 m,
- breadth B = 22.8 m,
- draught d = 9.14
- block coefficient CB = 0.563,
- Froude numer Fn = 0.2
- wavelength/ship length ratio λ/LBP = 1.

At the first stage, using formulas (15)–(20) the values of coefficients b_1, …, b_6 were calculated as:

$$b_1 = 152.5 \cdot 0.0038 - 0.3396 = 0.240 \tag{21}$$

$$b_2 = 22.8 \cdot 0.0240 - 0.3894 = 0.158 \tag{22}$$

$$b_3 = 9.14 \cdot 0.0602 - 0.2530 = 0.297 \tag{23}$$

$$b_4 = 0.563 \cdot 3.0675 - 1.5429 = 0.184 \tag{24}$$

$$b_5 = 0.2 \cdot 4.6948 - 0.4085 = 0.530 \tag{25}$$

$$b_6 = 1 \cdot 0.4425 - 0.0708 = 0.372 \tag{26}$$

Then, using formula (14), the values of coefficients a_1, …, a_6 were calculated as:

$$\begin{bmatrix} a_1 \\ a_2 \\ a_3 \\ a_4 \\ a_5 \\ a_6 \end{bmatrix} = \begin{bmatrix} 3.966 & -2.399 & 3.903 & -0.313 & 1.244 & 1.314 \\ -0.771 & 1.832 & -1.256 & -0.085 & 1.242 & 0.983 \\ -2.361 & 2.803 & -1.692 & 1.452 & 0.706 & 3.916 \\ -0.784 & -3.674 & -0.801 & 4.763 & -0.922 & 0.146 \\ -2.206 & 0.078 & -2.305 & -3.661 & -1.082 & -4.008 \\ 16.057 & -1.270 & 12.316 & 3.231 & 3.893 & 3.88 \end{bmatrix} \times \begin{bmatrix} 0.240 \\ 0.158 \\ 0.297 \\ 0.184 \\ 0.530 \\ 0.372 \end{bmatrix} - \begin{bmatrix} 4.608 \\ 0.783 \\ 3.792 \\ -0.399 \\ -1.865 \\ -0.395 \end{bmatrix} = \begin{bmatrix} 0.181 \\ -1.345 \\ -0.343 \\ 0.880 \\ 3.275 \\ 1.374 \end{bmatrix} \tag{27}$$

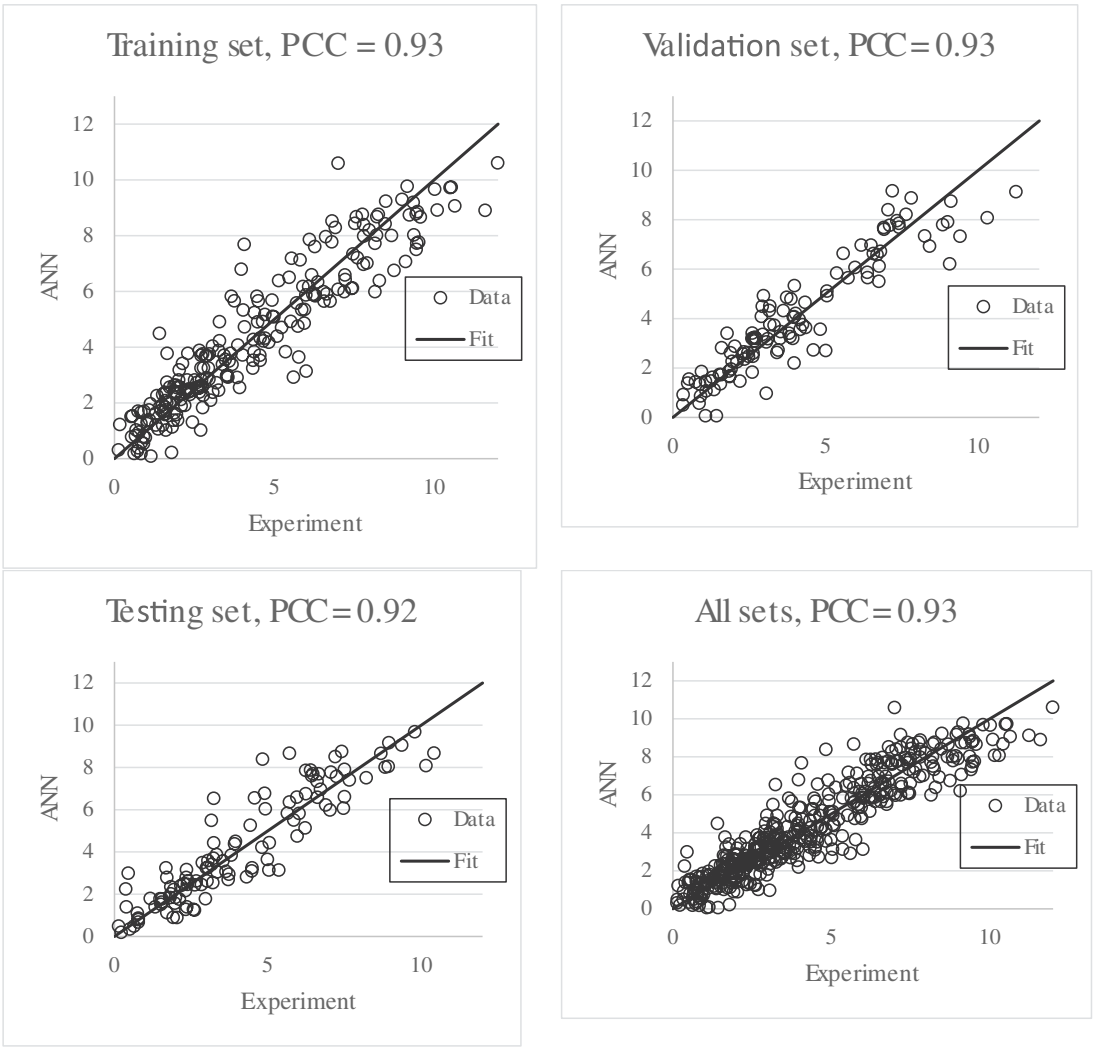

Fig. 4. Regression graphics presenting the developed network.

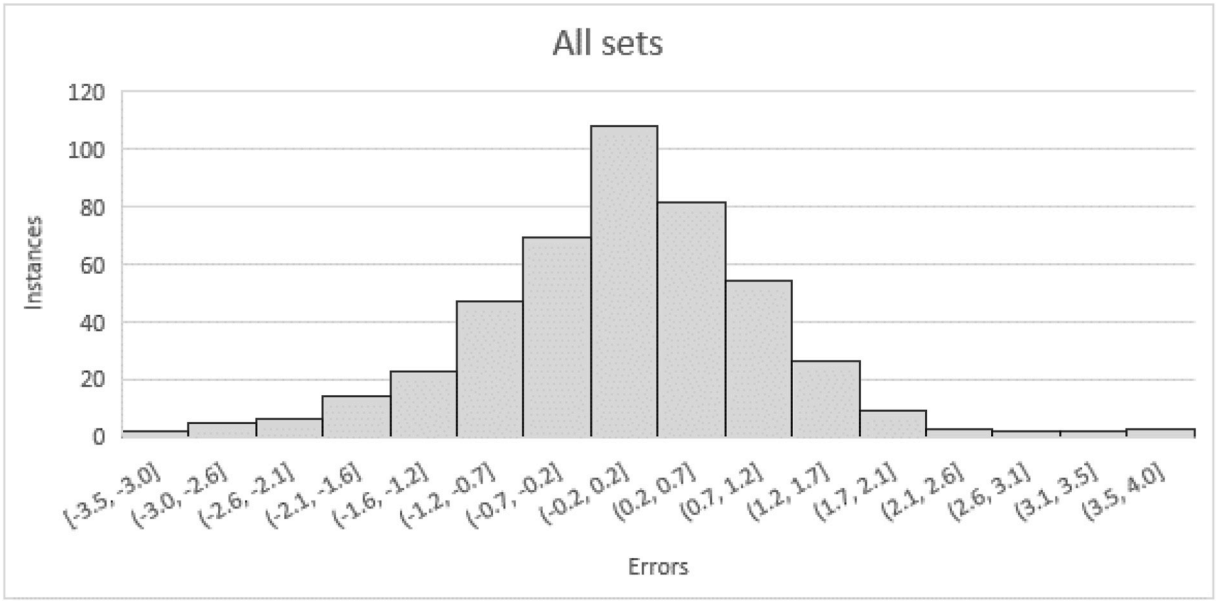

Fig. 5. Error histogram of developed ANN model.

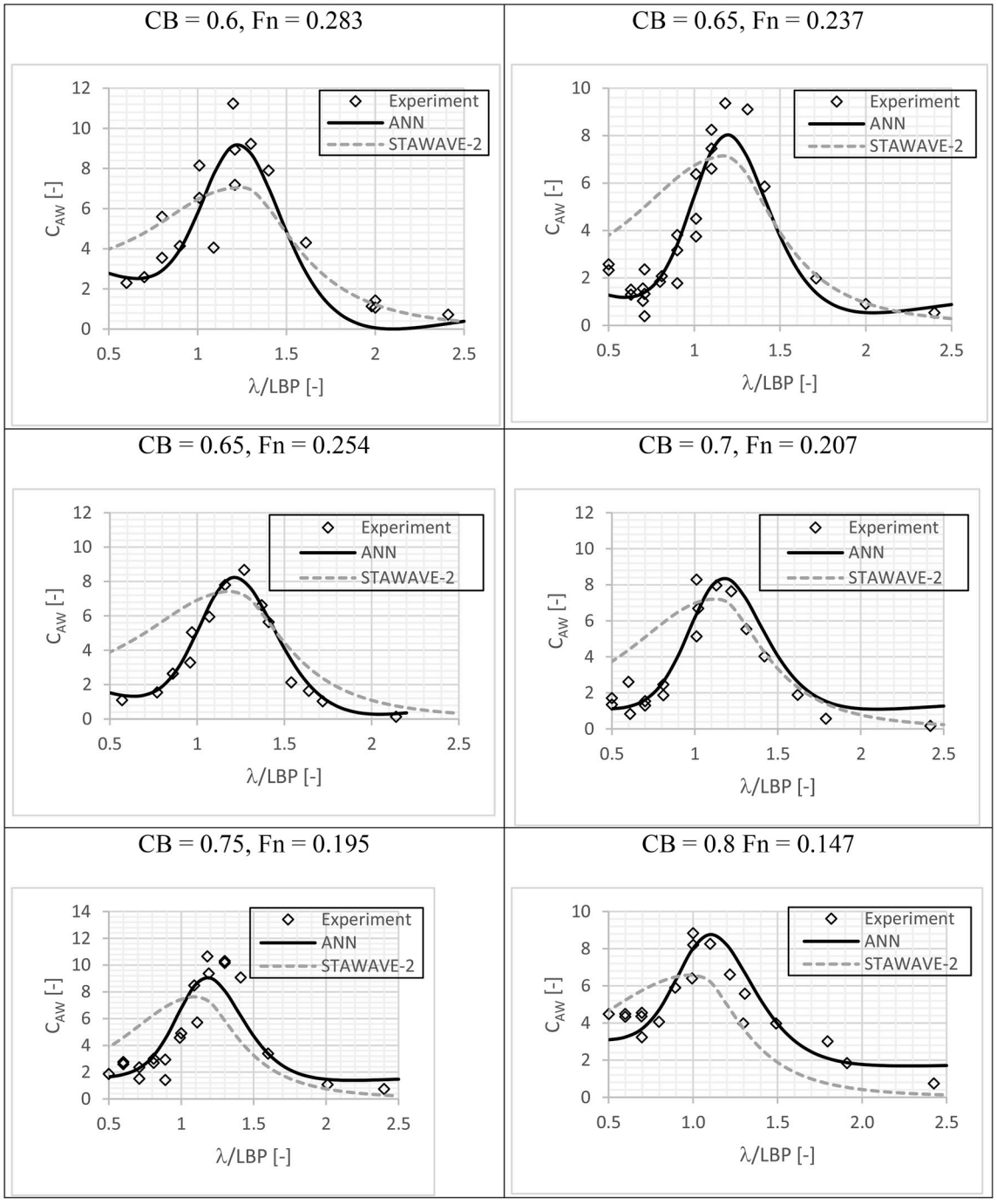

Fig. 6. Added resistance of Series 60 models in head waves, compared to model test measurements and calculations from the artificial neural network and STAWAVE-2.

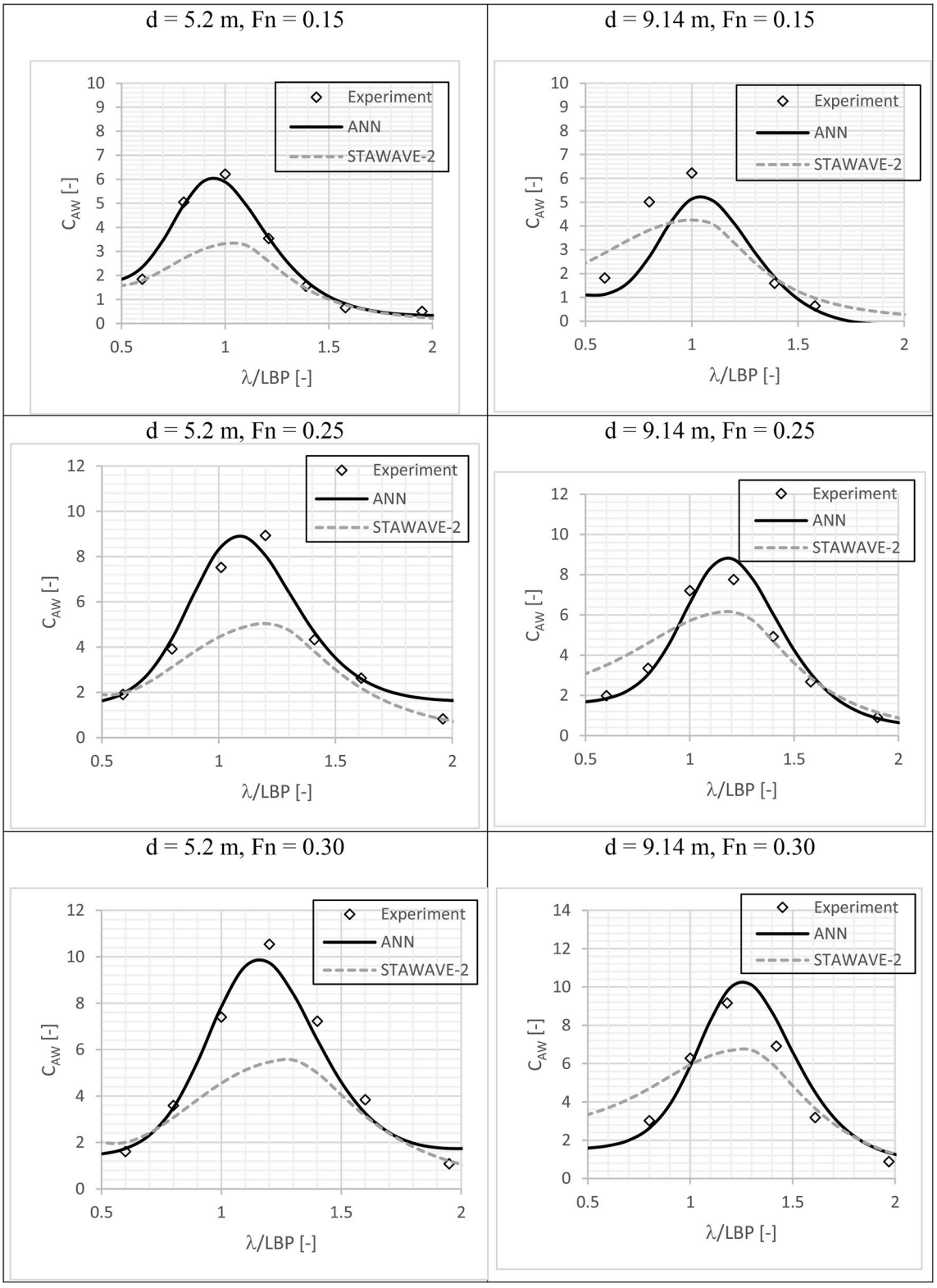

Fig. 7. Added resistance of "Van der Stel" in head waves, compared to model test measurements and calculations from the artificial neural network and STAWAVE-2.

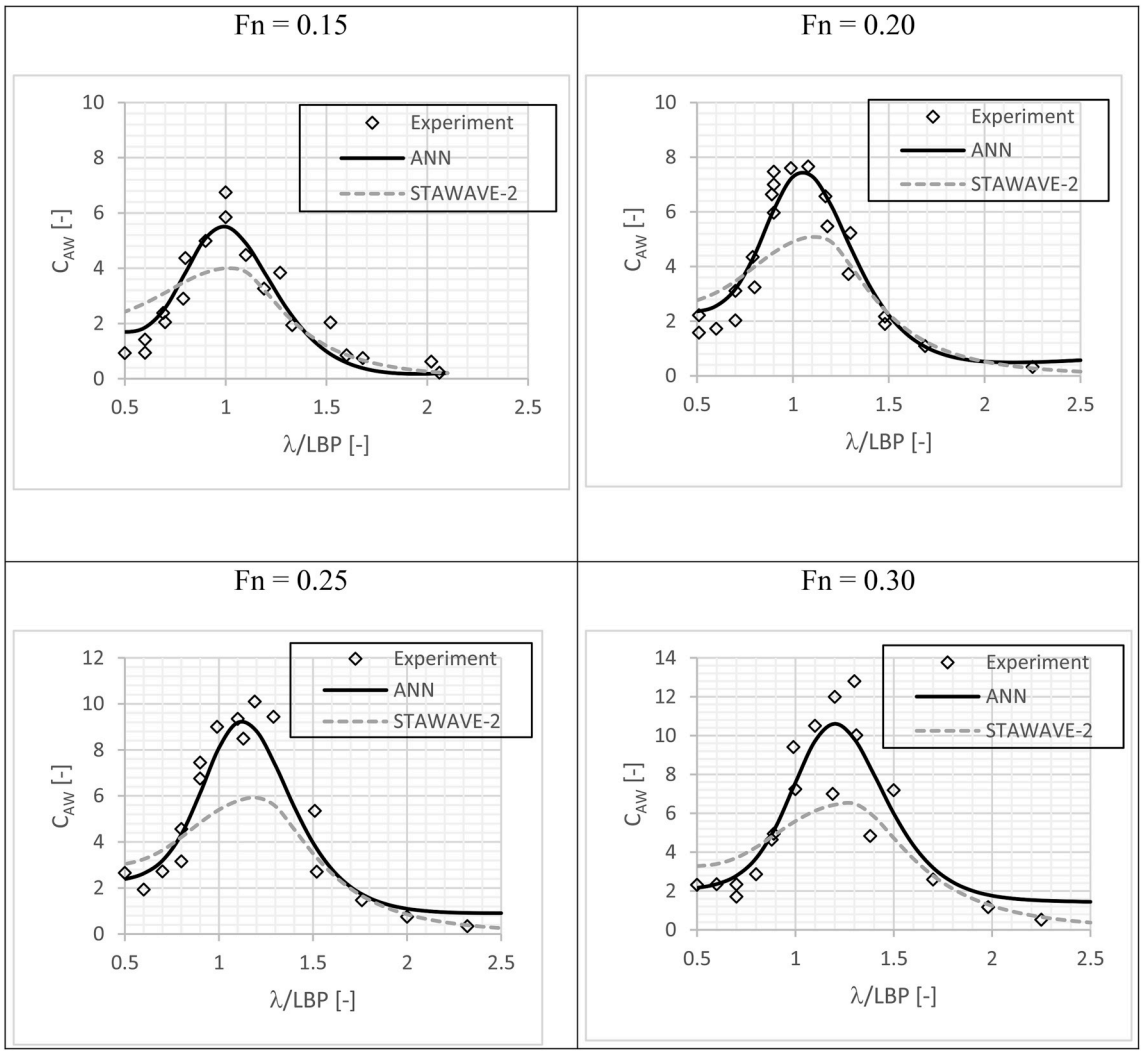

Fig. 8. Added resistance of an S-175 container ship in head waves, compared to model test measurements and calculations from the artificial neural network and STAWAVE-2.

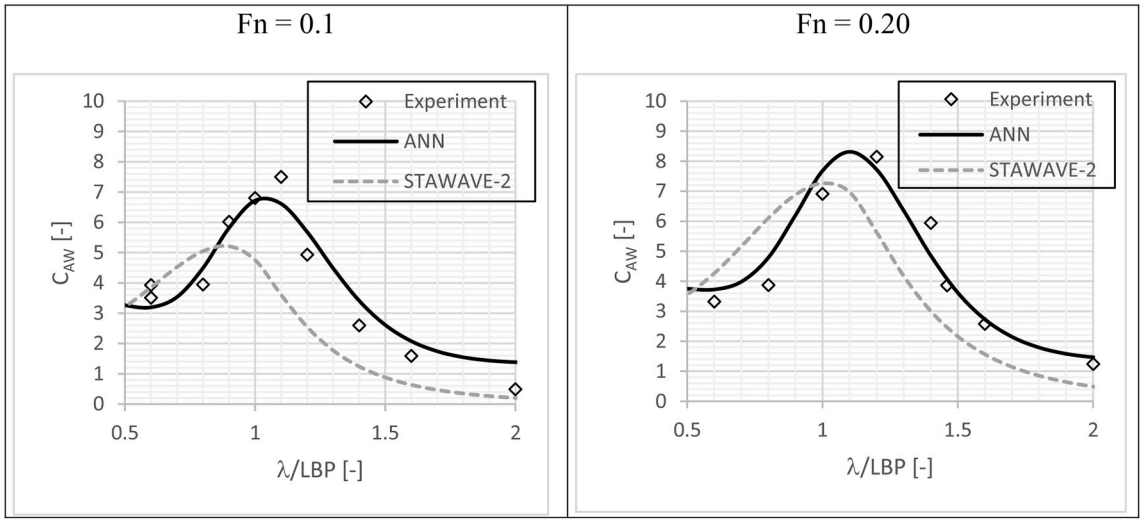

Fig. 9. Added resistance of a bulk carrier in head waves, compared to model test measurements and calculations from the artificial neural network and STAWAVE-2.

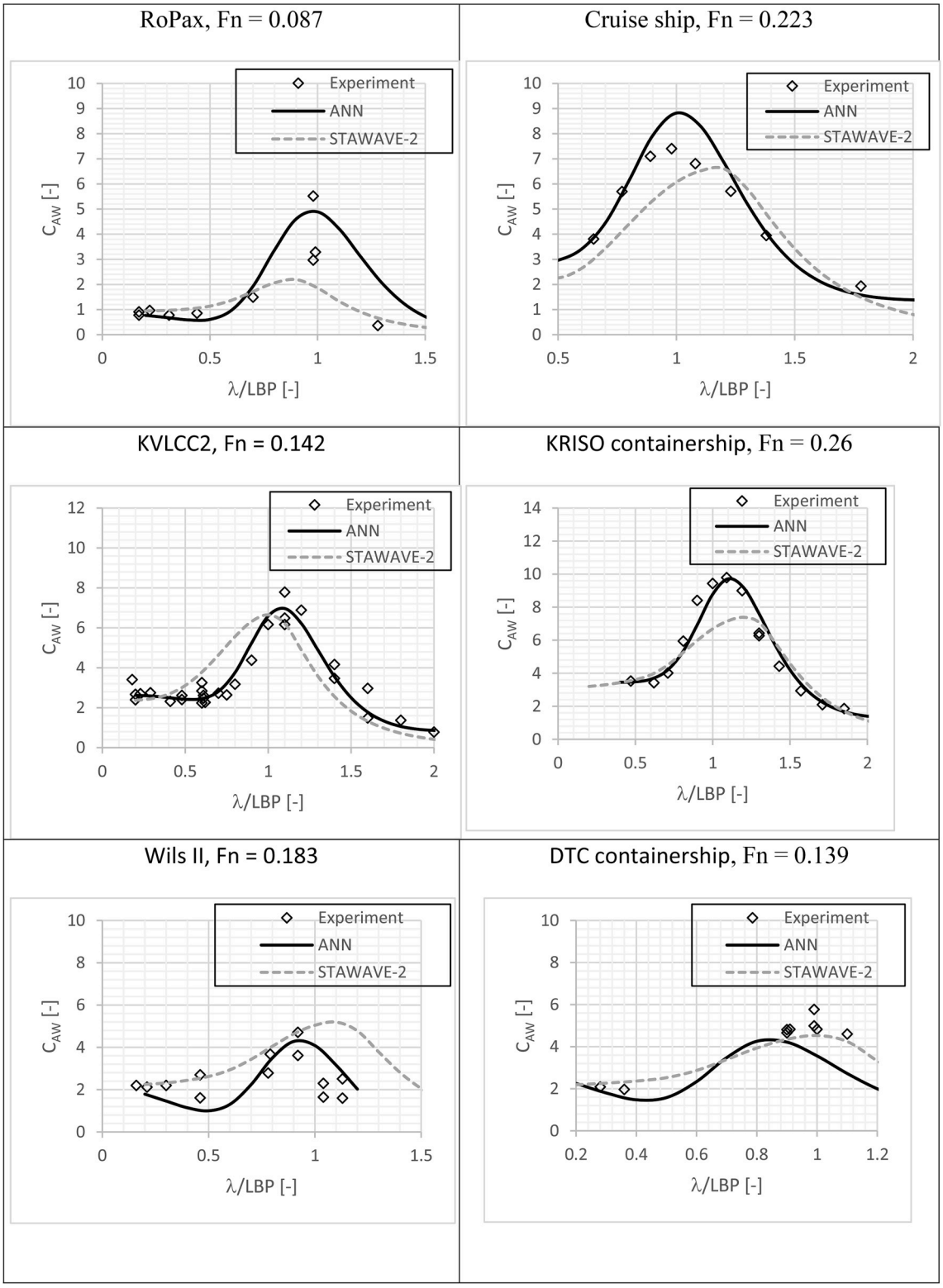

Fig. 10. Added resistance of selected ships in head waves, compared to model test measurements and calculations from the artificial neural network and STAWAVE-2.

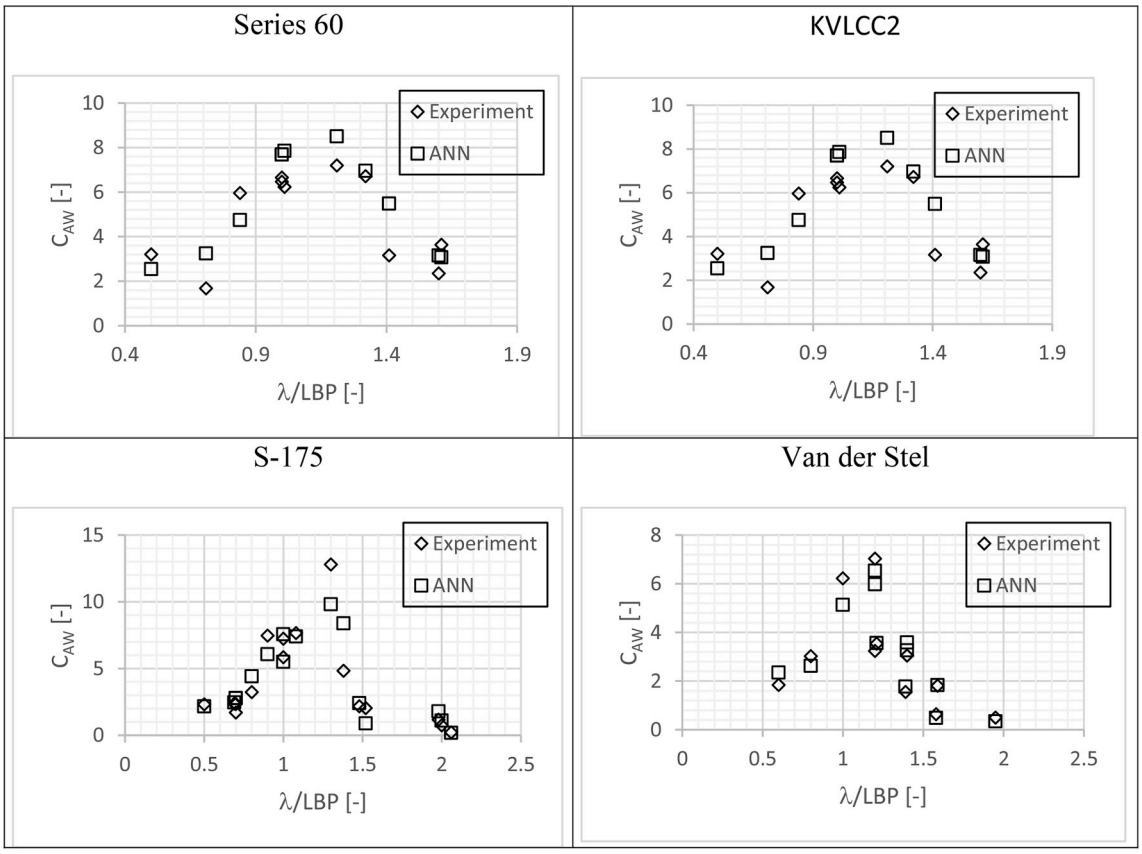

Fig. 11. A comparison of the values estimated when using the neural network with experiments by using only test data.

Placing the values of coefficients a_1, …, a_6 calculated using formula (27) to formula (13), we found the following column matrix A:

$$A = \begin{bmatrix} \frac{1}{1+e^{-a_1}} \\ \frac{1}{1+e^{-a_2}} \\ \frac{1}{1+e^{-a_3}} \\ \frac{1}{1+e^{-a_4}} \\ \frac{1}{1+e^{-a_5}} \\ \frac{1}{1+e^{-a_6}} \end{bmatrix} = \begin{bmatrix} \frac{1}{1+e^{-0.181}} \\ \frac{1}{1+e^{1.345}} \\ \frac{1}{1+e^{0.343}} \\ \frac{1}{1+e^{-0.88}} \\ \frac{1}{1+e^{-3.275}} \\ \frac{1}{1+e^{-1.374}} \end{bmatrix} = \begin{bmatrix} 0.545 \\ 0.207 \\ 0.415 \\ 0.707 \\ 0.964 \\ 0.798 \end{bmatrix} \tag{28}$$

Then, making use of Equation (12) the value of coefficient c was calculated:

$$c = [3.2352 \; -1.5865 \; -3.5529 \; -0.8379 \; -0.8081 \;\; 0.8799] \times \begin{bmatrix} 0.545 \\ 0.207 \\ 0.415 \\ 0.707 \\ 0.964 \\ 0.798 \end{bmatrix} + 1.23 = 0.522 \tag{29}$$

and making use of formula (11) we finally found:

$$C_{AW} = \frac{0.522 + 0.01087}{0.08361} = 6.37 \tag{30}$$

formula (30) represents the value of the added wave resistance coefficient as 6.37 for the assumed parameters.

6. Conclusions

An ANN model to predict an added wave resistance coefficient was obtained and found that the multilayer perceptron including 6 neurons in the input and hidden layers in each, and 1 neuron in the output layer. This was a useful tool for the prediction of added wave resistance.

This study showed that results provided good correlation with measured data. A large part of the difference between the measured and estimated value varied between −1.2 and + 1.2. Statistical analysis confirmed that the developed neural network had good generalization ability.

Table 3
The design characteristics of ship models not used at all in the development of the neural network, where: LBP – length between perpendiculars, B – breadth, d – draught, CB – block coefficient and Fn – Froude number.

Model	LBP [m]	B [m]	d [m]	CB [-]	Fn [-]	LBP/B	B/d	Data source
SR221C tanker	320	58	19.3	0.803	0.15	5.5	3.0	Kashiwagi et al. (2004) as cited in Liu et al. (2019)
Container ship	300	40	14	0.66	0.247	7.5	2.9	Tsujimoto et al. (2008)
Aframax tanker	239	44	13.6	0.835	0.154	5.4	3.2	Oh et al. (2015)
Product carrier	145.4	23.4	8	0.757	0.177	6.2	2.9	Li et al. (2016)

The developed formula (11) presented in this paper could have practical application at the preliminary design stage, specifically for ships characterized by design parameters similar to ships used in this research. But this formula might have two limitations. Firstly, formula (11) may be inaccurate in the design of an innovative ship. This results from the data used to train the network which was measured on standard ship hulls. Secondly, the neural network was developed using the model test data with limited parameter ranges. Therefore, the developed artificial neural network might only be used to estimate added wave resistance for ships with the following design characteristic ranges:

- length between perpendiculars LBP from 90 m to 335 m,
- breadth B from 16.25 m to 58 m,
- draught d from 4.2 to 20.8 m,
- block coefficient CB from 0.503 to 0.829,
- Froude number Fn from 0.087 to 0.3,
- LBP/B ratio from 5 to 7.5,
- B/d ratio from 2.5 to 4.5

and a wavelength/ship length ratio λ/LBP of 0.5–2.0.

The application of a developed network to calculate ship resistance with design characteristics outside these ranges could be associated with the risk of less accurate estimations. The B/d and LBP/B ratio narrow ranges may be a limitation in the development of neural network application.

Since wave heading is not an input variable, the method presented here is only valid for a long-crested head sea. This could be a significant limitation, especially for ships in service to asses their wave resistance in the seaway. However, for design purposes, there is little need to estimate wave resistance from all wave directions. A designer usually compares design variants, taking into account the resistance, only from the direction of the head wave. Therefore, the method presented in this study could be practical applied at the Preliminary design stage to compare and select optimal design variants.

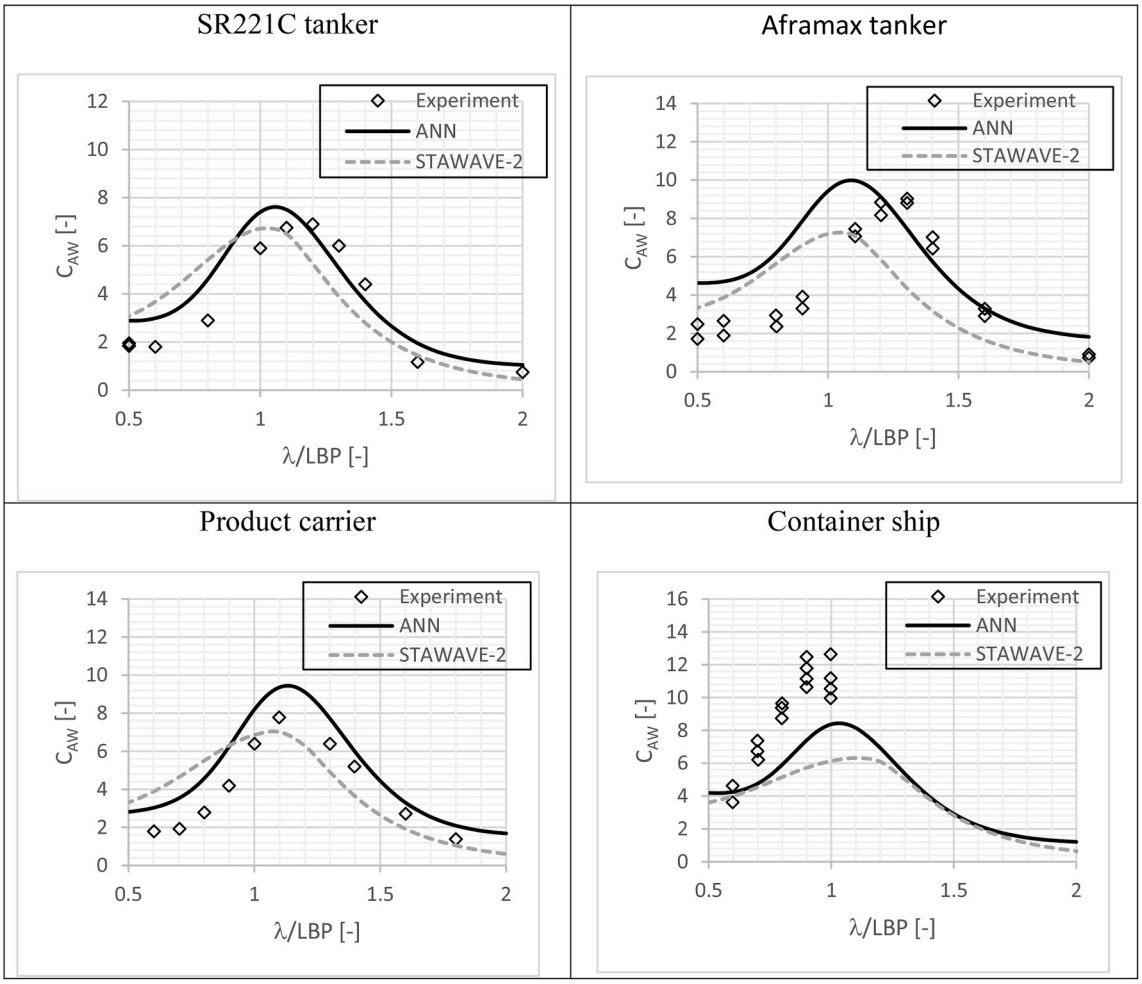

Fig. 12. A comparison of the values estimated when using the neural network and the STAWAVE-2 method with experiments for ships that were not used at all in the development of the neural network.

In general, the artificial neural network predicts added wave resistance effectively, even when the measured data set has large dispersion. This study suggests that with a large enough measurement data set it is might be possible to estimate the resistance for a ship of any hull shape and design characteristic through the use of an artificial neural network.

Declaration of competing interest

The authors declare that they have no known competing financial interests or personal relationships that could have appeared to influence the work reported in this paper.

Acknowledgment

This research outcome has been achieved under the research project No S/2/S/INM/16 financed from a subsidy of the Polish Ministry of Science and Higher Education for statutory activities.

References

Abramowski, T., 2013. Application of artificial intelligence methods to preliminary design of ships and ship performance optimization. Nav. Eng. J. 125 (3), 101–112.
Arribas, F., Pérez, 2007. Some methods to obtain the added resistance of a ship advancing in waves. Ocean Engineering 34, 946–955, 2007.
Bishop, C., 1995. Neural Networks for Pattern Recognition. University Press, Oxford.
Boom, H. van den, Huisman, H., Mennen, F., Jan/Feb. 2013. New Guidelines for Speed/Power Trials. SWZ/Maritime.
Broyden, C.G., 1970. The convergence of a class of double-rank minimization algorithms 1. General considerations. IMA J. Appl. Math. 6 (1), 76–90.
Cepowski, T., 2016. Approximating the added resistance coefficient for a bulk carrier sailing in head sea conditions based on its geometrical parameters and speed. Pol. Marit. Res. 23, 8–15. https://doi.org/10.1515/pomr-2016-0066.
Cepowski, T., 2008. Modelling of added wave resistance on the basis of the ship's design parameters. Computer Systems Aided Science and Engineering Work in Transport, Mechanics and Electrical Engineering (121), 39–46. Radom.
Chądzyński, W., 2001. Elements of Contemporary Design Methods of Floating Objects. Scientific Reports of Szczecin University of Technology (in Polish).
Ekinci, S., Celebi, U.B., Bal, M., Amasyali, M.F., Boyaci, U.K., 2011. Predictions of oil/chemical tanker main design parameters using computational intelligence techniques. Appl. Soft Comput. 11, 2356–2366.
FALTINSEN, O.M., MINSAAS, K.J., LIAPIS, N., 1980. SKJ?RDAL, S.: "prediction of resistance and propulsion of a ship in a seaway. In: Proceedings of the 13th ONR Symposium.
Fausett, L., 1994. Fundamentals of Neural Networks. Prentice Hall, New York.
Fletcher, R., 1970. A new approach to variable metric algorithms. Comput. J. 13 (3), 317–322.
Fujii, H., Takahashi, T., 1975. Experimental study on the resistance increase of a ship in regular oblique waves. Proc. 14th ITTC 4, 351–360.
GERRITSMA, J., BEUKELMAN, W., 1972. Analysis of the resistance increase in waves of a fast cargo-ship. Int. Shipbuild. Prog. 18 (217).
Goldfarb, D., 1970. A family of variable-metric methods derived by variational means. Math. Comput. 24 (109), 23–26.
Guo, B., Steen, S., 2010. Added resistance of a VLCC in short waves. In: Proc. 29th Int. Conf. on Ocean, Offshore & Arctic Engineering. OMAE 2010.
Gurgen, S., Altin, I., Ozkok, M., 2018. Prediction of main particulars of a chemical tanker at preliminary ship design using artificial neural network. Ships Offshore Struct. 13 (5), 459–465. https://doi.org/10.1080/17445302.2018.1425337.
Haykin, S., 1994. Neural Networks: A Comprehensive Foundation. Macmillan Publishing, New York.
ITTC, 2017. Recommended Procedures and Guidelines - Preparation, Conduct and Analysis of Speed/Power Trials. ITTC.
Joncquez, S.A.G., Bingham, H., Andersen, P., 2008. Validation of Added Resistance Computations by a Potential Flow Boundary Element Method, 27th Naval Hydrodynamics, Seoul, Korea.
Joosen, W.P.A., 1966. Added resistance of ships in waves. In: Proceedings of the 6th Symposium on Naval Hydrodynamics (Wasington,D.C).
Journee, J.M.J., 1976. Motions, Resistance and Propulsion of a Ship in Longitudinal Regular Waves. Ship Hydromechanics Laboratory, Delft University of Technology, The Netherlands.
Kadomatsu, K., 1988. Study on the Required Minimum Output of Main Propulsion Engine Considering Maneuverability in Rough Sea. PhD thesis. Ship Design Lab., Yokohama National University, Japan.
Kashiwagi, M., 2009. Impact of hull design on added resistance in waves- application of the enhanced unified theory. In: Proceedings of the 10th International Marine Design Conference. Trondheim, Norway, pp. 521–535.
Kashiwagi, M., Sugimoto, K., Ueda, T., Yamazaki, K., Arihama, K., Kimura, K., Yamashita, R., Itoh, A., Mizokami, S., 2004. An analysis system for propulsive performance in waves. J. Kansai Soc. Nav. Archit. Jpn. 241, 67–82.
Kim, K.H., Kim, Y., 2011. Numerical study on added resistance of ships by using a time-domain Rankine panel method. Ocean. Eng. 38, 1357–1367. https://doi.org/10.1016/j.oceaneng.2011.04.008.
Kuroda, M., Tsujimoto, M., Fujiwara, T., 2008. Investigation on components of added resistance in short waves. J. Jpn. Soc. Nav. Archit. Ocean Eng. 8, 171–176 (CrossRefView Record in ScopusGoogle Scholar).
Ley J, Sigmund S, el Moctar O. 2014. Numerical prediction of the added resistance of ships in waves. ASME. International Conference on Offshore Mechanics and Arctic Engineering, Volume 2: CFD and VIV ( ):V002T08A069. doi:10.1115/OMAE2014-24216.
Li, C., Ma, X., Chen, W., Li, J., Dong, G., 2016. Experimental investigation of self propulsion factor for a ship in regular waves. Shipbuild China 57 (1), 1–8.
Liu, S.K., Papanikolaou, A., 2016. Fast approach to the estimation of the added resistance of ships in head waves. Ocean. Eng. 112, 211–225. https://doi.org/10.1016/j.oceaneng.2015.12.022.
Liu, S., Papanikolaou, A., 2016. On the prediction of the added resistance of large ships in representative seaways. Ships Offshore Struct. 12, 690–696, 2016.
Liu, S., Papanikolaou, A., 2019. Approximation of the added resistance of ships with small draft or in ballast condition by empirical formula. Proc. Inst. Mech. Eng. M J. Eng. Marit. Environ. 233 (1), 27–40. https://doi.org/10.1177/1475090217710099.
Liu, S., Shang, B., Papanikolaou, A., 2019. On the resistance and speed loss of full type ships in a seaway. Ship Technol. Res. 66 (3), 163–181. https://doi.org/10.1080/09377255.2019.1613294.
Liu, S., Shang, B., Papanikolaou, A., Bolbot, V., 2016. Improved formula for estimating added resistance of ships in engineering applications. J. Mar. Sci. Appl. 15 (4), 442–451. https://doi.org/10.1007/s11804-016-1377-3.
Maruo, H., 1960. The drift of a body floating on waves. J. Ship Res. 4 (3), 1–10.
Nakamura, S., 1976. Added resistance and propulsive performance of ships in waves. In: International Seminar on Wave Resistance. The Society of Naval Architects of Japan, Japan.
Newman, J.N. (1967)The drift force and moment on ships in waves. J. Ship Res.. Volume 11, Issue 1, Pages 51-60.
Oh, S., Yang, J., Park, S.-H., 2015. Computational and experimental studies on added resistance of Aframax-class tankers in head seas. J Soc Nav Archit Korea 52 (6), 471–477.
Papanikolaou, A., 2014. Ship Design: Methodologies of Preliminary Design. Springer, Dordrecht.
Patterson, D., 1996. Artificial Neural Networks. Prentice Hall, Singapore.
Rawson, K.J., Tupper, E.C., 2001. Basic Ship Theory: Ship Dynamics and Design. Butterworth-Heinemann.
Sadat-Hosseini, H., Wu, P., Carrica, P., Kim, H., Toda, Y., Stern, F., 2013. CFD verification and validation of added resistance and motions of KVLCC2 with fixed and free surge in short and long head waves. Ocean Engineering 59, 240–273.
SALVESEN, N., 1978. Added resistance of ships in waves. J. Hydronautics 12 (1), 23–34. https://doi.org/10.2514/3.63110.
Shanno, D.F., 1970. Conditioning of quasi-Newton methods for function minimization. Math. Comput. 24 (111), 647–656.
Shepherd, J., 1997. Second-Order Methods for Neural Networks. Springer, New York.
Simonsen, C.D., Otzen, J.F., Nielsen, C., Stern, F., 2014. CFD prediction of added resistance of the KCS in regular head and oblique waves. In: Proceedings of 30th Symposium on Naval Hydrodynamics. Hobart, Australia.
Söding, H., Shigunov, V., Schellin, T.E., el Moctar, O., 2014. A rankine panel method for added resistance of ships in waves. J. Offshore Mech. Arct. Eng. https://doi.org/10.1115/1.4026847.
Sprenger, F., Maron, A., Delefortrie, G., Hochbaum, A., Fathi, D., 2015. Mid-term review of Tank test results. SHOPERA Deliverable D3 2.
Strøm-Tejsen, J., Yeh, H.Y.H., Moran, D.D., 1973. Added resistance in waves. Trans. - Soc. Nav. Archit. Mar. Eng. 81, 109–143.
TIBCO Software Inc, 2017. Statistica (data analysis software system). version 13. http://statistica.io.
Tsujimoto, M., Kuroda, M., Shibata, K., Takagi, K., 2008. A practical correction method for added resistance in waves. J. Jpn. Soc. Nav. Archit. Ocean Eng. 8, 177–184. https://doi.org/10.2534/jjasnaoe.8.177.
Watson, D.G.M., 1998. Practical Ship Design, vol. 1. Elsevier Science.
Cepowski, T., 2019. AddResistance (Windows/MAC OS)", Mendeley Data, v1 (1.0) (accessed 6 November 2019).
Lazarus, 2019. The professional Free Pascal RAD IDE (2.0.0) (accessed 19 April 2019).